

# Estimating Optimal Regions for Improvement in Range Acquisition from a Single Point of View

Phillip Curtis and Pierre Payeur

School of Electrical Engineering and Computer Science

University of Ottawa

Ottawa, ON, Canada

[pcurtis, ppayeur]@eecs.uottawa.ca

**Abstract**—It is well established that acquiring large amount of data can quickly lead to important data management challenges where processing capabilities become saturated and preempt full usage of the information available for autonomous systems to make educated decisions. While sub-sampling offers a naïve solution for reducing dataset dimension, it does not capitalize on the knowledge available in already acquired data to selectively drive further acquisition over the most significant regions. This paper discusses the development of a probabilistic occupancy grid based algorithm to automatically establish which regions within a single point of view from a range sensor would provide the most improvement if further acquisitions were made. The algorithm, which is independent of the sensor used, is validated with range data acquired from the popular Kinect multi-modal imaging sensor.

**Index Terms**—probabilistic occupancy grid, range sensing, 3D imaging, smart sensing, selective sensing, Kinect.

## I. INTRODUCTION

With the continuous improvement of semiconductor manufacturing technologies, production of sensors has dropped in cost, while at the same time improving their overall quality and the amount of data they produce. This has led to a larger number of sensors being used in numerous applications, such as cell phone cameras, entertainments systems with Microsoft Kinect, security applications, and robotic platforms. Interpreting all of this rich and dense information from a wide variety of sensors is a complex task, which is known as the 'Big Data Challenge' [1, 2].

While this work does not deal with the related issues of handling and combining data across multiple sensors and sharing of that data, it addresses the sub-issue of 3D data acquisition. One way to tackle the Big Data Challenge consists of minimizing the amount of data points acquired in a range image. A promising approach to achieve this goal aims at identifying regions in the scene which need a higher density of points, and other areas which do not. In the context of this work, range acquisition from a single point of view of the sensor is considered to properly evaluate performance without dependency on data registration considerations. By performing this analysis, the data can be effectively compressed at acquisition time, while ensuring both an appropriate level of coverage of the overall scene and the quality of the 3D model created. This is accomplished through an original algorithm that builds on probabilistic occupancy grids to determine regions which provide the most overall benefit for the acquisition.

Firstly, reviews of relevant techniques for determining where to scan next in a multi-view setup, techniques for determining optimal scanning patterns, and approaches for intelligent adaptive sensing from a single point of view are presented. An introduction to probabilistic occupancy grids is then discussed. Next, the algorithm being proposed is developed. Finally experimental results are presented and analyzed before concluding remarks are made.

## II. LITERATURE REVIEW

Other works in the past have dealt with the issue of identifying to which location a sensor should be moved in order to improve the coverage and quality of the model of a scene, while minimizing the amount of separate acquisitions required. These approaches are well known as next best view (NBV) algorithms.

Connolly [3], through his previous usage of octrees generated from multiple views [4], realized that determining optimal viewing vectors based on the current knowledge of the scene would improve the overall time required to model a scene. He describes two different methods for determining the NBV: by determining the view which would reveal the most 'unseen' nodes in the octree (the planetarium algorithm), and by summing together the normals of the faces of nodes that are common to both 'unseen' and 'empty' nodes in order to produce a viewing vector which sees the greatest amount of potentially visible 'unseen' nodes (the normal algorithm).

The goal of eliminating occlusions to drive the NBV process was investigated by several researchers [5, 6, 7, 8]. Morooka *et al.* [9] define a discretized shell around a region to be modeled in order to limit the number of possible viewing vectors, which allows the use of lookup tables to optimize the entire process. Mackinnon *et al.* [10] use a laser range sensor which provides several additional fields of data in order to derive a quality metric for each acquisition point in order to drive the NBV process to optimize the quality of the overall model.

There has also been works that have looked into optimal fixed scanning patterns for several scenarios. Ho and Saripalli [11] have investigated scanning patterns for autonomous underwater vehicles (AUV) which attempt to maximize coverage and quality, while minimizing energy use from the AUV propulsion system. English *et al.* [12] use three different patterns, a Lissajous, a rosette, and a spiral scanning pattern, along with an adaptive algorithm to swap between them depending on the characteristics and objects detected in the

scene, with the goal of optimizing the estimation of position and orientation.

Adaptive and intelligent sensing for range acquisition was previously investigated by Cretu *et al.* [13], who determine regions which require higher resolution acquisition based upon an initial course scan, from within a single point of view. Their method uses a neural gas network to determine where varying features and edges are located by training the network over a short period, which produces clusters of points in regions where there are features. The resulting clusters are then analyzed, and regions with higher density of clusters, which correspond to regions in space where there are more potential features, are re-acquired at a higher resolution.

Shih *et al.* [14] develop three different techniques to guide a non-uniform data acquisition process from a single point of view. In the first two approaches, an initial scan of the object is made. This object is then subdivided in a hierarchal tree-type fashion, with error between actual values at the leaf nodes and the estimated values at those points calculated from the next layer up being used to determine if new points within each sub-division is acquired. The difference between the first two approaches is that the first approach uses plane fitting over regularly shaped sections, such as rectangles and triangles, while the second approach uses curve fitting. The third and final approach determines the optimal non-uniform scanning pattern for a particular object based upon a CAD model, by first performing a virtual acquisition, and then using a local adjustment algorithm to move points around until an optimal placement occurs where the points cease to move. The resulting point locations correspond to the optimal scanning pattern for that particular object.

In robotic navigation and path planning however, many researchers do not tend to rely on meshed surface models, but rather on volumetric models. In particular, probabilistic occupancy grids developed by Elfes [15], which are a Bayesian updated form of the occupancy octrees that Connolly developed in [4], provide a framework to take into account the uncertainty of the measurements acquired from the sensors on a robotic platform. They also define probabilistic rules for merging data acquired from various views into a single model. The probability being used is the probability that a particular cell is occupied given a set of measurements. A conversion between probabilistic occupancy grids and regular occupancy grids can be made by thresholding the probabilities contained within each node, where a low probability corresponds to empty space, high probability corresponds to occupied, and a middling probability is unknown. Payeur *et al.* in [16] develop a closed-form solution to optimize the application of probabilistic occupancy grids for 3-D modeling of dynamic scenes. By using probabilistic occupancy grids, a robot can be made to only move around in regions where it is sufficiently confident that it is empty, and has an inherent method of increasing confidence of knowledge about a region by repeatedly acquiring data in that region until it is sufficient enough to navigate through.

### III. PROPOSED ALGORITHM WITH IMPROVEMENT MEASURE

Most range sensors available, such as laser range finders, stereo vision, and structured light systems, are projective based. Consequently, these sensors have a focal point through which

their data is collected, allowing the modeling of the collected data in a spherical coordinate system, without worrying about self occlusions within the data. Hence, the proposed algorithm uses a spherical probabilistic occupancy grid.

The starting point of the algorithm uses the closed-form equations developed by Payeur *et al.* [16], which yields a sensor occupancy probability distribution function (OPDF),  $P_s(\rho, \theta, \varphi | \bar{\rho}, \bar{\theta}, \bar{\varphi}, \sigma_\rho, \sigma_\theta, \sigma_\varphi)$ , defined in eq. (1). The variables  $\rho, \theta, \varphi$  correspond to the depth, azimuth, and elevation values in a spherical occupancy grid,  $\bar{\rho}, \bar{\theta}, \bar{\varphi}$  correspond to the measured location using the sensor, and  $\sigma_\rho, \sigma_\theta, \sigma_\varphi$  correspond to the standard deviation of the sensor measurements along the respective spherical axes.

$$P_s(\rho, \theta, \varphi | \bar{\rho}, \bar{\theta}, \bar{\varphi}, \sigma_\rho, \sigma_\theta, \sigma_\varphi) = \frac{1}{2} \left( 1 + e^{-\left( \frac{2((\rho-\bar{\rho})+2\sigma_\rho)}{\sigma_\rho} + \frac{(\theta-\bar{\theta})^2}{\sigma_\theta^2} + \frac{(\varphi-\bar{\varphi})^2}{\sigma_\varphi^2} \right)} \right)^{-1} + \frac{1}{3} e^{-\left( \frac{(\rho-\bar{\rho})^2}{\sigma_\rho^2} + \frac{(\theta-\bar{\theta})^2}{\sigma_\theta^2} + \frac{(\varphi-\bar{\varphi})^2}{\sigma_\varphi^2} \right)} \quad (1)$$

The Bayesian rule for updating the value of the probability of occupancy for any voxel based upon the current occupancy probability, as well as the OPDF of the acquisition at a particular point is shown in eq. (2).  $v_i$  is the voxel in which the point  $(\rho, \theta, \varphi)$  is located,  $a_k$  is the acquisition of the  $k^{\text{th}}$  data point  $(\bar{\rho}, \bar{\theta}, \bar{\varphi})$  with the sensor standard deviations of  $(\sigma_\rho, \sigma_\theta, \sigma_\varphi)$ ,  $P_o^t(v_i)$  is the conditional probability that voxel  $v_i$  is occupied at time  $t$ , and  $P_s(v_i | a_k)$  is the probability that voxel  $v_i$  is occupied given a measurement from the sensor with values of  $a_k$ .

$$P_o^{t+1}(v_i | P_o^t(v_i), P_s(v_i | a_k)) = \frac{P_o^t(v_i) P_s(v_i | a_k)}{P_o^t(v_i) P_s(v_i | a_k) + (1 - P_o^t(v_i))(1 - P_s(v_i | a_k))} \quad (2)$$

Based upon the Bayesian relationship described in eq. (2), it is possible to express the estimated future probability of occupancy based upon the current probability of occupancy, as well as the possible acquisition at a particular point through the OPDF function. In order to maximize the knowledge of whether or not space is occupied or empty, and whether acquiring a depth value along a particular ray in the spherical space will maximize the knowledge about the scanned area, a measure of improvement in the knowledge of the probability of occupancy is required.

To perform this over the entire 3D occupancy grid is computationally expensive, and unneeded since a single point of view is considered here. Within the probabilistic occupancy grid acquired from a single point of view, there will be a surface of highest probability determined by the surface of the closest object in any given direction within the field of view of the range sensor, taking into account that behind any object the volume is occluded from the sensor and its probability of occupancy remains 50% (unknown) by default. This surface of highest probability is created by determining the depth at which the highest probability of occupancy occurs for each azimuth

and elevation value represented in the grid. Taking into account this piece of information, the problem is reduced from 3D to 2D, and the computational requirements of the calculation of the Bayesian update in order to determine the improvement of acquiring a point of data is reduced to calculations along the surface of highest probability. Furthermore, by limiting the sensor's OPDF region of influence by truncating it to a region within a multiple of the sensor's respective standard deviations along the azimuth and elevation axes, only a limited number of voxel's need to have their estimates of improvement updated after the acquisition of another point.

To determine an estimate of improvement of the knowledge of occupancy of a region a simulated acquisition,  $\hat{a}_j$ , is made along the ray  $(\theta_j, \varphi_j)$ , with a depth,  $\rho_j$ , corresponding to that of the most probabilistic surface. The current probability of occupancy in the corresponding voxel in spherical coordinates is subtracted from the new probability of occupancy of the same voxel assuming that the simulated acquisition is merged into the occupancy grid. This defines the estimated improvement,  $imp(v_i | P_o^t(v_i), P_s(v_i | \hat{a}_j))$ , as follows:

$$imp(v_i | P_o^t(v_i), P_s(v_i | \hat{a}_j)) = \frac{P_o^t(v_i) P_s(v_i | \hat{a}_j)}{P_o^t(v_i) P_s(v_i | \hat{a}_j) + (1 - P_o^t(v_i)) (1 - P_s(v_i | \hat{a}_j))} - P_o^t(v_i) \quad (3)$$

The change in the probability of a single voxel when a new acquisition is made, is not enough to determine the overall improvement in the confidence of occupancy. Rather the total summation of this improvement happening over all voxels which the acquisition at  $\hat{a}_j$  affects, according to the truncated OPDF, must be performed. Furthermore only the voxels currently belonging to the surface of highest probability are used, as defined in eq. (4). The resulting cumulative improvement,  $imp(\hat{a}_j)$ , can be negative. Such a negative improvement can be interpreted as uncertainty in the degree of overall improvement in the region, which can be due to variable sampling densities as well as depth transitions.

$$imp(\hat{a}_j) = \sum_{v_i \in \text{truncated OPDF}} imp(v_i | P_o^t(v_i), P_s(v_i | \hat{a}_j)) \quad (4)$$

As the distribution of  $P_s(v_i | \hat{a}_j)$  is the probability distribution of the possible sensor acquisition along the most probable surface for the purpose of calculating improvement, only the voxels around the region of support provided by the standard deviation of the sensor model need to be used. This effectively makes the improvement calculation a non-linear rectangular filter in 2D. Furthermore, by keeping track of which elements of the surface of highest probabilistic occupancy have changed after the addition of a point, the number of points updated after an acquisition can also be limited to the size of the sensors OPDF, within a multiple of its standard deviation.

The evaluation of the proposed method is performed using range images acquired from the popular Microsoft Kinect platform, which has a variety of sensors integrated, including a RGB camera, a microphone array, and a depth sensor which uses an IR camera and an IR projector to generate a structured light pattern. Data acquisition was accomplished using the open source OpenNI drivers, with the depth sensor resolution set at 640x480. The Kinect's depth sensor has a 57° horizontal, and a 43° vertical field of view [17], and provides reliable data between 0.8m and 3.5m [17, 18, 20] with a maximum range of 0.5m - 9m [19, 20]. The spatial resolution at 2m depth is 3 mm along the horizontal and vertical axis, and 1cm along the depth axis.

While there have been studies [20] that discuss the error model of the depth measurements of the Kinect, they do not report on the error along the other axes. Therefore the quantization noise is used for the Kinect sensor error model for the azimuth and elevation axes. This tends not to have a dramatic effect, since any measurement error along the X and Y axes incorporates itself to error along the depth axis due to the triangulation nature of the depth measurement. The depth noise model used is a combination of the measurement noise developed and the quantization noise [20]. The maximum variance along the azimuth, elevation, and depth within the supported region, which is 0.8m - 5.0m, is used as the parameters for the OPDF. This yields variances of  $\sigma_\theta^2 = \sigma_\varphi^2 = 1.88 \times 10^{-7} \text{rad}^2$  and  $\sigma_\rho^2 = 2.23 \times 10^3 \text{mm}^2$ . The number of bins used in the spherical probabilistic occupancy grid for the azimuth and elevation axes is the same as the resolution of the sensor, that is 640x480. The number of discrete bins along the depth axis is 512. The region of support used for the OPDF is two standard deviations.

The depth images acquired are from an underground parking garage, which provides a large but controlled environment which typically is not found in traditional laboratories, as well as from a low height above ground in order to simulate what a mobile robot would perceive. A non-linear color mapping has been performed on the improvement maps such that the differences between improvements is clearer, and the mapping from the  $imp(\hat{a}_j)$  parameter of eq. (4) is illustrated in Fig. 1.

The depth, occupancy, and improvement maps are produced at 640x480, and each pixel represents a ray through the centre of a bin of the spherical probabilistic occupancy grid. Fig. 2a shows a scene imaged by the Kinect's RGB camera and displaying two pillars in the parking garage with empty parking spaces. Fig. 2b shows the depth of the most probabilistic surface. Black pixels correspond to 0m depth from the sensor, that is ray projections where there was no depth information provided by the sensor. White pixels represent the maximum depth of 5m and beyond, and gray values represent the intermediate depth between 0m and the maximum depth. Fig. 2c shows the probability of occupancy of the most probabilistic surface in the scene, where black represents empty space (probability of 0% occupancy), middle gray value represents unknown occupancy (probability of 50% occupancy), and the lighter gray values map higher probability of occupancy. Note that the black regions in Fig. 2b correspond to the middle grey regions in Fig. 2c since they remain unknown (50%) as they

were not imaged by the depth sensor, due to occlusion created by the pillar between the IR projector and the IR camera over certain surfaces, or because of too large distance. Finally, Fig. 2d shows the estimated improvement measure computed along the surface with highest probability. Red regions represent the areas where the most improvement is to be achieved with extra data acquisition, which are the areas where there is no information available yet from the sensor. The green regions are areas where no or little improvement can be obtained. They essentially correspond to regions that are located beyond the sensor's maximum depth of field. The blue regions correspond to areas where the improvement is negative, and they lie on transitions between objects that are at different depths. The yellow and orange regions correspond to areas where there are a higher density of measurements already available in the probabilistic occupancy grid within the depth of field of the sensor. Note that the striped pattern visible in Fig. 2c and 2d is due to the non-linear mapping between the uniform spherical occupancy grid spacing, and the uniform Cartesian grid

spacing, which results in a higher density of point being inserted further away from the center of the occupancy grid, with an approximately equal density of points at roughly half way between the center of the grid and its edges. An intelligent sensing application can be developed through prioritizing regions based on expected improvement, such that regions that are orange/red have a higher priority of being captured in future acquisitions than green/yellow regions. Furthermore if the desire is to acquire higher confidence on severe transitions, then regions of negative improvement can be re-acquired.

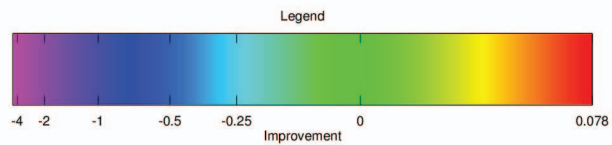


Fig. 1. Color map for the estimated improvement measure.

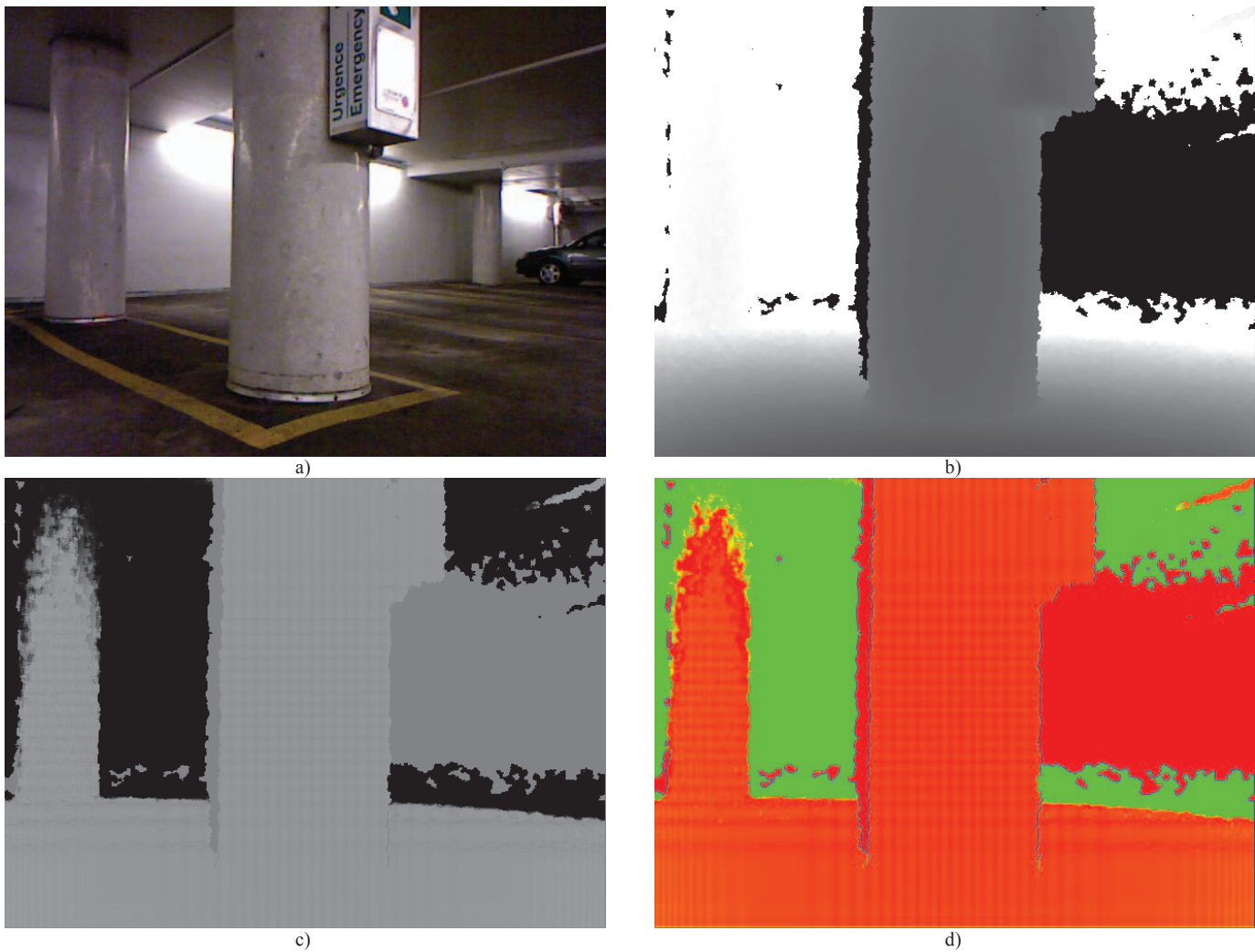
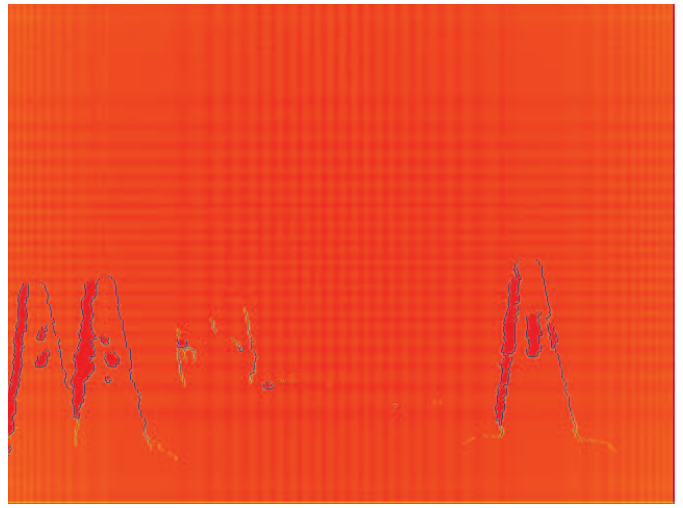


Fig. 2. Parking garage scene a) RGB image, b) depth of the surface with highest occupancy probability, c) probability of occupancy for the surface with highest probability, and d) improvement estimate over the surface with highest probability.

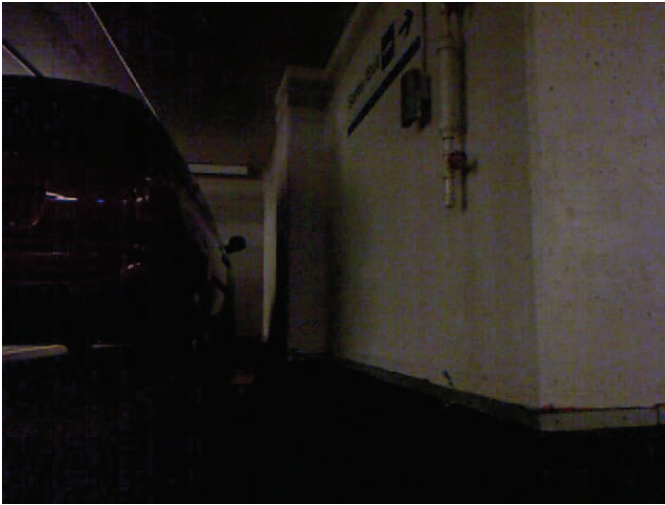


a)

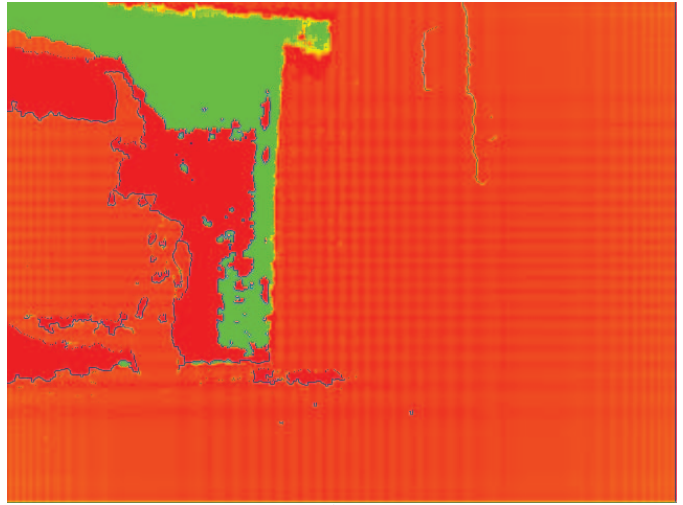


b)

Fig. 3. Cluttered scene a) RGB image, b) improvement estimate over the surface with highest probability.



a)



b)

Fig. 4. Scene of vehicle and wall a) RGB image, b) improvement estimate over the surface with highest probability.

Table 1. Mean timing data for probability occupancy grid generation and improvement calculations over 10 runs.

Data Set	# Points	Mean Insertion Time (sec)	Mean Time for Improvement Calculation (sec)	Mean Time for Improvement per Point (sec/point)	Mean Percentage of Total Time for Improvement Calculation (%)
Fig. 2	254060	29.46	1.47	5.80E-06	4.76
Fig. 3	307200	31.84	1.82	5.92E-06	5.41
Fig. 4	279299	29.72	1.65	5.90E-06	5.25

Fig. 3 illustrates a cluttered scene with some traffic cones and a recycling bin with a few items inside. As seen in Fig. 3b, applying the proposed framework, the region where the most improvement can be achieved by further acquisitions is determined as the areas of occlusion between the IR projector on the Kinect and its infrared camera, as well as the regions with reflective strips on the cones, over which the Kinect depth sensor did not acquire many data points. The transition regions between objects of different depths are again marked by a blue outline representing negative improvement in probability of occupancy. The latter characteristic indicates that such an

improvement map can also prove useful to support segmentation of objects in the depth map.

Fig. 4 is interesting since it shows a narrow region between a vehicle and a wall. The regions of highest estimated improvement correspond to the rear glass of the vehicle, the lens of the rear lights, and regions of occlusion. There are also regions of moderate potential improvement (yellow) where points at the edge of the depth of field (5m) are integrated into the probabilistic occupancy grid.

The results in Table 1 were obtained on a computer with an Intel Core i7 2630QM processor with 8GB of RAM running Windows 7 64 bit operating system, with the application being

compiled as a 64-bit application. The turbo-boost capability of the processor caused the chip to operate at 2.6 GHz during the computation of the results. The algorithm was executed 10 times, and the mean execution time was calculated for each of the three data sets included in this paper. The mean insertion time is the mean time that was required to insert all the points of the depth image into the probabilistic occupancy grid. The mean time for improvement calculation is the mean execution time required to calculate the improvement values for all the affected locations due to all the points that were inserted into the probabilistic occupancy grid. The timing data shows that to calculate the estimated improvement,  $imp(\hat{a}_j)$ , takes approximately 5.8-6.0  $\mu$ s per point to calculate, which is between 4.76% - 5.41% of the total execution time.

## V. CONCLUSIONS

The proposed method to estimate improvement of the probability of occupancy in a model built progressively from a series of 3D data acquisitions is an effective technique to selectively and automatically determine which regions of a scene require the acquisition of supplementary data. It can also serve as a tool to determine when to stop acquiring more data. Moreover, the approach can readily be used to detect regions where there is greater uncertainty in the estimation of improvement in the model due to sparse sampling or a sharp depth transition region, by paying attention to regions of negative improvement. The technique is adapted to operate from a single point of view of the sensor, while requiring no other information aside from a measurement error model of the sensor. It takes full advantage of the potential offered by probabilistic occupancy grids for mapping complex environments, and it performs sufficiently fast to support real-time directed acquisition with any type of range sensor.

The technique described in this paper is meant to serve as a stage in an intelligent sensing pipeline, where a decision process involving the 1-step improvement calculation presented here would be required. Additionally, the results from the improvement map can be used in 3D segmentation, as sharp discontinuities are outlined by a region of negative improvement.

## ACKNOWLEDGMENTS

The authors would like to acknowledge the support of Ontario Centres of Excellence (OCE) and Natural Sciences and Engineering Research Council of Canada (NSERC) toward this research.

## REFERENCES

[1] "Big Data - Wikipedia, the free encyclopedia," [Online]. Available: [http://en.wikipedia.org/wiki/Big\\_data](http://en.wikipedia.org/wiki/Big_data). [Accessed 19 07 2012].

[2] L. G. Weiss, "Autonomous Robots in the Fog of War," *IEEE Spectrum*, pp. 30-34, 56-57, Aug. 2011.

[3] C. I. Connolly, "The Determination of Next Best Views," *IEEE International Conference on Robotics and Automation*, pp. 432-435, Mar. 1985.

[4] C. I. Connolly, "Cumulative Generation of Octree Models from Range Data," *IEEE International Conference on Robotics and Automation*, pp. 25-32, Mar. 1984.

[5] K. Klein and V. Sequeira, "The View-Cube: An Efficient Method of View Planning for 3D Modelling from Range Data," *IEEE Workshop on Applications of Computer Vision*, pp. 186-191, Palm Spring, CA, Dec. 2000.

[6] M. K. Reed, P. K. Allen and I. Stamos, "3-D Modeling from Range Imagery," in *IEEE International Conference on Recent Advances in 3-D Digital Imaging and Modeling*, pp. 76-83, May 1997.

[7] V. Sequeira, J. G. M. Goncalves and M. I. Ribeiro, "Active View Selection for Efficient 3D Scene Reconstruction," *IEEE Proc. of the International Conference on Pattern Recognition*, Vienna, Austria, vol. 1, pp. 815-819, Aug 1996.

[8] J. Maver and R. Bajcsy, "Occlusions as a Guide for Planning the Next View," *IEEE Transactions on Pattern Analysis and Machine Intelligence*, vol. 15, no. 5, pp. 417-433, May 1993.

[9] K. Morooka, H. Zha and T. Hasegawa, "Computations on a Spherical View SPace for Efficient Planning of Viewpoints in 3-D Object Modeling," *IEEE International Conference on 3-D Digital Imaging and Modeling*, pp. 138-147, Oct. 1999.

[10] D. MacKinnon, V. Aitken and F. Blais, "Adaptive Laser Range Scanning using Quality Metrics," *IEEE Instrumentation and Measurement Technology Conference*, Victoria, BC, pp. 348-353, May 2008.

[11] C. Ho and S. Saripalli, "Where Do You Sample? - An Autonomous Underwater Vehicle Story," *IEEE International Symposium on Robot and Sensors Environments*, Montreal, QC, pp. 119-124, Sep. 2011.

[12] C. English, G. Okouneva, P. Saint-Cyr, A. Choudhuri and T. Luu, "Real-Time Dynamic Pose Estimation Systems in Space: Lessons Learned for System Design and Performance Evaluation," *International Journal of Intelligent Control and Systems*, vol. 16, no. 2, pp. 79-96, 2011.

[13] A.-M. Cretu, P. Payeur and E.-M. Petriu, "Selective Range Data Acquisition Driven by Neural Gas Networks," *IEEE Transactions on Instrumentation and Measurement*, vol. 58, no. 8, pp. 2634-2642, 2009.

[14] C. S. Shih, L. A. Gerhardt, C.-C. Williams, C. Lin, C.-H. Chang, C.-H. Wan and C.-S. Koong, "Non-uniform Surface Sampling Techniques for Three-dimensional Object Inspection," *Optical Engineering*, vol. 47, no. 5, 053606, May 2008.

[15] A. Elfes, "Occupancy Grids: A Probabilistic Framework for Robot Perception and Navigation", Ph.D. dissertation, Dept. of Electrical and Computer Engineering, Carnegie Mellon University, Pittsburg, PA., 1989.

[16] P. Payeur, P. Hébert, D. Laurendeau and C. M. Gosselin, "Probabilistic Octree Modeling of a 3-D Dynamic Environment," *International Conference on Robotics and Automation*, vol. 2, pp. 1289-1296, Albuquerque, NM, Apr. 1997.

[17] Microsoft, "Kinect for Windows Sensor Components and Specifications," Microsoft, [Online]. Available: [http://msdn.microsoft.com/en-us/library/jj131033\(d=printer\).aspx](http://msdn.microsoft.com/en-us/library/jj131033(d=printer).aspx). [Accessed 19 07 2012].

[18] B. Klug, "AnandTech - Microsoft Kinect: The AnandTech Review," AnandTech, 12 09 2010. [Online]. Available: <http://www.anandtech.com/show/4057/microsoft-kinect-the-anandtech-review/2>. [Accessed 18 07 2012].

[19] PrimeSense, "PrimeSense 3D Sensor Data Sheet," [Online]. Available: <http://primesense.com/en/press-room/resources/file/4-primesense-3d-sensor-data-sheet>. [Accessed 17 07 2012].

[20] K. Khoshelham, "Accuracy Analysis of Kinect Depth Data," *ISPRS Workshop Laser Scanning 2011*, Calgary, AB, Aug. 2011.